

## Auxiliary field diffusion Monte Carlo calculation of properties of oxygen isotopes

S. Gandolfi,<sup>1,\*</sup> F. Pederiva,<sup>1,2,†</sup> S. Fantoni,<sup>2,3,‡</sup> and K. E. Schmidt<sup>4,§</sup>

<sup>1</sup>Dipartimento di Fisica dell'Università di Trento, and INFN, Gruppo Collegato di Trento via Sommarive 14, I-38050 Povo, Trento, Italy

<sup>2</sup>INFN DEMOCRITOS National Simulation Center Via Beirut 2/4, I-34014 Trieste, Italy

<sup>3</sup>International School for Advanced Studies, SISSA, Via Beirut 2/4, I-34014 Trieste, Italy

<sup>4</sup>Department of Physics and Astronomy, Arizona State University, Tempe, Arizona 85287, USA

(Received 5 August 2005; published 7 April 2006)

The ground state and some low-lying excited states of oxygen isotopes  $^{18}\text{O}$ – $^{22}\text{O}$  were simulated by means of auxiliary field diffusion Monte Carlo techniques. We performed the calculations by replacing the  $^{16}\text{O}$  core with a mean-field self-consistent potential we computed by using Skyrme interactions. The external neutrons were included in the Monte Carlo calculations, building a wave function with the orbitals computed in the self-consistent external potential. The shell considered was the  $1D_{5/2}$ . The  $NN$  interactions employed included tensor, spin-orbit, and three-body forces. While absolute binding energies are too deep compared with those of experimental data, the differences between the energies for nearly all isotopes and excitations are in very good agreement with the experiments. The exception is the  $4^+$  state of the  $^{18}\text{O}$  isotope, which shows a larger discrepancy.

DOI: [10.1103/PhysRevC.73.044304](https://doi.org/10.1103/PhysRevC.73.044304)

PACS number(s): 21.60.Ka, 21.30.-x, 27.20.+n, 27.30.+t

### I. INTRODUCTION

The structure of stable nuclei is generally dominated by shell effects that can be nearly completely explained by the single-particle picture of the system. However, it has been found experimentally, by means of fragmentation of heavy-ion beams [1–4], that neutron rich nuclei show features that seem to go beyond the standard shell model. For example, it was observed that the neutron drip line for O and F isotopes has a sudden change. This has been interpreted as a clear sign that many-body effects in this regime cannot be treated as a perturbation of the one-particle picture, but become relevant in determining the overall structure. Theoretical discussions of the insurgence of a new magic number at  $N = 16$  have recently been developed by means of mean-field calculations [5] and antisymmetrized molecular dynamics [6]. Recently Green's function Monte Carlo (GFMC) calculations with the use of realistic interactions have been performed. In this case the nuclei (all oxygen isotopes) were approximated as  $N$  neutrons in a potential well built to reproduce the density of protons in the  $^{16}\text{O}$  core [7].

In this paper we propose an analysis of heavy oxygen isotopes in the  $1D_{5/2}$  shell based on the auxiliary field diffusion Monte Carlo (AFDMC) [8] method, which, while relying on a shell-model picture for the treatment of the core, fully includes the effects of quantum correlations and of realistic interactions (in particular AV8' + U1X) in the treatment of the off-shell neutrons. This scheme was already employed in part in past works [9] in which the  $NN$  interactions considered were the Hasegawa–Nagata [10] and the Volkov [11]. In our case the  $^{16}\text{O}$  core is replaced with the self-consistent potential well generated by a self-consistent calculation with Skyrme forces. The orbitals yielded are then used to construct a

correlated antisymmetric wave function that is then employed as a starting point and an importance function for projecting the ground-state energy. This scheme tries to exploit the fact that self-consistent calculations partially include effects from quantum correlations and provide a better starting point for exact calculations with realistic interactions. Similar methods using density functional techniques to generate starting wave functions are commonly used in quantum Monte Carlo calculations of the electronic structure of molecules and solids [12]. Our study was not limited to the ground-state energies, but was also extended to some low-lying excited states.

The plan of the paper is as the follows. In the next section we describe the Hamiltonian used in our calculations. A brief outline of the AFDMC technique is given in Sec. III. Results for oxygen isotopes in the  $1D_{5/2}$  shell are discussed in Sec. IV. The last section is devoted to conclusions and future perspectives.

### II. HAMILTONIAN

The ground-state properties of the oxygen isotopes are computed starting from a nonrelativistic Hamiltonian of the following form:

$$\begin{aligned} \hat{H} &= T + V_1 + V_2 + V_3 \\ &= - \sum_i \frac{\hbar^2}{2m} \nabla_i^2 + \sum_i V_{\text{ext}}(\vec{r}_i) + \sum_{i<j} v_{ij} + \sum_{i<j<k} V_{ijk}. \end{aligned} \quad (1)$$

The one-body potential  $V_{\text{ext}}$  describes the  $^{16}\text{O}$  core, which in our calculations is replaced with a self-consistent potential we obtained by Hartree-Fock (HF) calculations using Skyrme forces.

The two-body  $NN$  interaction employed, which in our model acts among only the off-shell neutrons, belongs to the Urbana-Argonne  $v_l$  potentials [13,14]:

$$v_l = \sum_{i<j} \sum_{p=1}^l v_p(r_{ij}) \mathcal{O}^{(p)}(i, j), \quad (2)$$

\*Electronic address: [gandolfi@science.unitn.it](mailto:gandolfi@science.unitn.it)

†Electronic address: [pederiva@science.unitn.it](mailto:pederiva@science.unitn.it)

‡Electronic address: [fantoni@sissa.it](mailto:fantoni@sissa.it)

§Electronic address: [kevin.schmidt@asu.edu](mailto:kevin.schmidt@asu.edu)

truncated to include only the following eight operators ( $v'_8$ ):

$$O^{p=1,8}(i, j) = (1, \vec{\sigma}_i \cdot \vec{\sigma}_j, S_{ij}, \vec{L}_{ij} \cdot \vec{S}_{ij}) \times (1, \vec{\tau}_i \cdot \vec{\tau}_j), \quad (3)$$

where the operator  $S_{ij} = 3\vec{\sigma}_i \cdot \hat{r}_{ij}\vec{\sigma}_j \cdot \hat{r}_{ij} - \vec{\sigma}_i \cdot \vec{\sigma}_j$  is the tensor operator and  $\vec{L}_{ij} = -i\hbar\vec{r}_{ij} \times (\vec{\nabla}_i - \vec{\nabla}_j)/2$  and  $\vec{S}_{ij} = \hbar(\vec{\sigma}_i + \vec{\sigma}_j)/2$  are the relative angular momentum and the total spin for the pair  $ij$ , respectively. For neutrons  $\vec{\tau}_i \cdot \vec{\tau}_j = 1$ , and we are left with an isoscalar potential.

The  $v'_8$  potential is a simplified version of the  $v_{18}$  potential, having the same isoscalar parts of  $v_{18}$  in all  $S$  and  $P$  waves, as well as in the  ${}^3D_1$  channel and its coupling to the  ${}^3S_1$ . It is semirealistic in the sense that it does not fit the Nijmegen  $NN$  data at a confidence level of  $\chi^2/N_{\text{data}} \sim 1$ , as  $v_{18}$  does. However, the difference between  $v_{18}$  and  $v'_8$  is rather small for densities smaller than or of the order of the nuclear matter equilibrium density  $\rho_0 = 0.16 \text{ fm}^{-3}$ , and it can be safely added perturbatively. The  $v'_8$  potential should be considered as a *realistic* homework potential, and it has been used in a number of calculations on light nuclei [15,16], symmetric nuclear matter [17], neutron matter [18], spin-polarized neutron matter [19]. For isotopes heavier than  ${}^{19}\text{O}$ , a three-body Urbana IX (UIX) potential [15] has been included. Details of the treatment of this term within the AFDMC method can be found elsewhere [20].

### III. METHODS

#### A. Auxiliary field diffusion Monte Carlo method

The AFDMC method is an extension of the diffusion Monte Carlo (DMC) method to deal with spin-dependent Hamiltonians. The quadratic dependence of these Hamiltonians on the spin-operators is taken care of by sampling auxiliary variables, which serve to linearize such dependence through Hubbard–Stratonovich transformations. A detailed discussion of the method can be found in Refs. [18,21]. Here we limit ourselves to briefly outlining the method for the case of a pure neutron system and the  $v'_6$  interaction.

The  $v'_6$  two-body potential can be separated into a spin-independent part and a spin-dependent part:

$$V = V^{\text{SI}} + V^{\text{SD}},$$

$$V^{\text{SD}} = \sum_{i,j} \sigma_{i\alpha} A_{i\alpha;j\beta} \sigma_{j\beta},$$

where the elements of the matrix  $A$  are given by the proper combinations of the components  $v_p$  in Eq. (2). Latin indices, like  $i$  and  $j$ , are used for particles, while the Greek ones, like  $\alpha$  and  $\beta$ , refer to the Cartesian components of the operators. We use the summation convention that all repeated Greek indices are summed from 1 to 3.

Because  $A_{i\alpha;j\beta} = 0$  the  $3N \times 3N$  matrix  $A$  has real eigenvalues and eigenvectors, defined by

$$\sum_j A_{i\alpha;j\beta} \psi_n^{j\beta} = \lambda_n \psi_n^{i\alpha}. \quad (4)$$

The spin-dependent potential can therefore be written in terms of such eigenvalues and eigenvectors in the

following form:

$$V^{\text{SD}} = \frac{1}{2} \sum_n \left[ \sum_{i,j} \sigma_{i\alpha} \psi_n^{i\alpha} \lambda_n \psi_n^{j\beta} \sigma_{j\beta} \right]. \quad (5)$$

If one defines new  $N$ -body spinorial operators as

$$O_n = \sum_i \sigma_{i\alpha} \psi_n^{i\alpha}, \quad (6)$$

the spin-dependent potential becomes

$$V^{\text{SD}} = \frac{1}{2} \sum_{n=1}^{3N} \lambda_n O_n^2. \quad (7)$$

In the short-time limit we can decompose the imaginary time propagator of the diffusion process, which projects the ground state out of a trial wave function in the following way:

$$e^{-H\Delta\tau} \sim e^{-T\Delta\tau} e^{-V_c\Delta\tau} e^{-V^{\text{SD}}\Delta\tau}, \quad (8)$$

where  $V_c = \sum V_{\text{ext}}(r_i) + V^{\text{SI}}$  is the spin-independent part of the interaction. The propagation accounting for the kinetic and  $V_c$  operators gives rise to the usual drift-diffusion scheme of DMC. The spin-dependent two-body potential part  $e^{-V^{\text{SD}}\Delta\tau}$  is handled by use of the following Hubbard–Stratonovich transformation:

$$e^{-\frac{1}{2}\lambda_n O_n^2 \Delta\tau} = \frac{1}{\sqrt{2\pi}} \int_{-\infty}^{+\infty} dx_n e^{-\frac{x_n^2}{2} - \sqrt{-\lambda_n \Delta\tau} x_n O_n}, \quad (9)$$

with

$$e^{-V^{\text{SD}}\Delta\tau} \sim \prod_n e^{-\frac{1}{2}\lambda_n O_n^2 \Delta\tau}, \quad (10)$$

where the commutators among the  $O_n$  are neglected; this requires us to keep the time step  $\Delta\tau$  small.

In Eq. (9) the quadratic dependence on the spin operators is transformed into a linear expression that corresponds to a rotation in the spin space. For each eigenvalue  $\Psi_n^{i\alpha}$  a value of  $x_n$  is sampled, and the current spinor value for each particle is multiplied by the set of matrices given by the transformation in Eq. (9).

The spin-orbit and three-body potentials can be treated within the same scheme. It is important to note that, while the spin-orbit potential is already linear in the spin operator, it is necessary to eliminate spurious terms from the simple linearization of the propagator in order to take into account corrections at order  $\Delta\tau$ . This leads to additional two- plus three-body contributions, which can be treated as additional interaction terms. The AFDMC algorithm is implemented as usual, with a propagation in imaginary time of a population of walkers  $|R, S\rangle$  according to the propagator in relation (8) with the standard drift-diffusion procedure. In addition, one has to sample the  $x_n$  auxiliary variables given in Eq. (9) to rotate the spinors. After that, all the weight factors are computed; they are combined to evaluate a new value of  $\langle \Psi | R, S \rangle$ .

To avoid the fermion sign problem that is due to the antisymmetric character of the wave function, a path constraint is introduced. If the real part of  $\langle \Psi | R, S \rangle$  is negative, the walker is included in the evaluation of the mixed and growth energies, but then is dropped from the population. In general, the

importance sampling makes the number of dropped walkers very small. In our calculations here the number of node crossings is of the order of 1%.

### B. Wave function

The wave function used as the importance and projection function for the DMC algorithm has the following form:

$$\Psi(R, S) = F_J(R)D(R, S), \quad (11)$$

where  $R \equiv (\vec{r}_1, \dots, \vec{r}_N)$  and  $S \equiv (s_1, \dots, s_N)$ . The spin assignments  $s_i$  consist of giving the spinor components, namely,

$$s_i \equiv \begin{pmatrix} u_i \\ d_i \end{pmatrix} = u_i |\uparrow\rangle + d_i |\downarrow\rangle,$$

where  $u_i$  and  $d_i$  are complex numbers. The Jastrow correlation operator is given by

$$F_J = \prod_{i < j} f_J(r_{ij}), \quad (12)$$

and

$$D(R, S) = \mathcal{A} \prod_{i=1}^N \phi_{n,j,m_j}(\vec{r}_i, s_i), \quad (13)$$

is the Slater determinant of one-body spin-space orbitals:

$$\phi_{n,j,m_j}(\vec{r}, \vec{\sigma}) = \Psi_{n,j}(\vec{r}) Y_{l,m_l}(\theta, \phi) \xi_{s,m_s}. \quad (14)$$

We obtained the radial components by solving the HF problem with the Skyrme forces, which also provide the external potential well that describes the closed  $^{16}\text{O}$  core. The yielded radial functions are written in the  $j, m_j$  base, so we obtained the single-particle wave function by coupling the spherical harmonics with the spin by using the Clebsh-Gordan coefficients. In  $^n\text{O}$ ,  $n = 18-22$  isotopes, neutrons fill only the orbitals in the  $1D_{5/2}$  shell except for the isotope  $^{19}\text{O}$ , for which it is necessary to put some neutrons also in the  $1D_{3/2}$  in order to build the ground state of correct symmetry.

One obtains the many-body states by coupling the single-particle angular momentum by constructing eigenstates of total angular momentum  $J = j_1 + \dots + j_N$  with  $N = 2-6$ ; for the states with an even number of neutrons, the ground state has  $J = 0$ , while for odd neutron numbers, the ground state has total angular momentum  $J = 5/2$ . These states are in general written in terms of a sum of Slater determinants whose coefficients are determined by the symmetry of the state. Each determinant is evaluated at the current values of the positions and spin assignments of the nucleons in the walker  $|R, S\rangle$ .

The same procedure is used for the construction of the excited states, always limiting the choice of the single-particle orbitals to the shell  $1D_{5/2}$ .

The Jastrow function  $f_J$  has been taken as the scalar component of the Fermi Hyper-Netted Chain at the Single Operator Chain level (FHNC/SOC) correlation operator  $\hat{F}_{ij}$  that minimizes the energy per particle of neutron matter at density  $\rho = 0.16 \text{ fm}^{-3}$  [22]. The Jastrow part of the function in our case has the role only of reducing the overlap of nucleons and therefore reducing the energy variance. Since it does not change the phase of the wave function, it does not influence

TABLE I. Two sets of Skyrme's parameter used to perform variational calculations of energy,  $t_0$  (MeV fm<sup>3</sup>),  $t_1$  (MeV fm<sup>5</sup>),  $t_2$  (MeV fm<sup>5</sup>),  $t_3$  (MeV fm<sup>6</sup>),  $W_0$  (MeV fm<sup>5</sup>), and  $x_0$ .

Force	$t_0$	$t_1$	$t_2$	$t_3$	$x_0$	$W_0$
I	-1057.3	235.9	-100.0	14463.5	0.56	120.0
II	-1169.9	585.6	-27.1	9331.1	0.34	105.0

the computed energy value in projections methods. For this reason the Jastrow function has not been further optimized for our calculations.

In our calculations we neglected contributions for the  $2S_{1/2}$  orbital despite the expectation of significant mixing of this level in the states of isotopes considered. However, the fact that the AFDMC gives results for the energy differences in very good agreement with experimental data indicates that the effects of the mixing are not extremely significant. The inclusion of contributions from the  $2S_{1/2}$  orbital also gives rise to major technical difficulties. In fact, the component along this orbital tends to be projected over the more bound  $1S_{1/2}$  state, giving rise to a nonphysical density for the external neutrons. This difficulty also prevented us from extending our calculations to higher mass isotopes to the drip line.

### C. Determination of the HF well

An important issue in this calculation is the choice of the Skyrme force parameters to be used to generate the effective-HF potentials included in the Hamiltonian for AFDMC calculations. The use of a self-consistent potential well makes the single-particle part of the importance function essentially parameterless. In the absence of an efficient variational procedure, it was important to establish that this choice of orbitals could be in general reasonable, if not optimal.

Skyrme forces cannot be related directly to the realistic  $NN$  interaction used in our calculation. We must therefore establish a criterion for discriminating among different choices. As a first step we computed the variational energy of the closed-shell isotope  $^{22}\text{O}$  on the correlated Slater determinants we obtained by using different sets of parameters in the Skyrme Hamiltonian, but using the full Hamiltonian with potential  $V8'+\text{UIX}$ . In particular we tried the Skyrme I and Skyrme II [23] forces, whose parameters are given in Table I.

The expectation value of the Hamiltonian (reported in Table II) considerably differs in the two cases. This is mainly

TABLE II. Ground-state variational energies of  $^{22}\text{O}$  starting from two different types of single-particle effective potential and orbitals, obtained with different types of Skyrme's parameters. We report the total energy, the kinetic energy (calculated with the Jackson-Feenberg [24] and Pandharipande-Bethe [25] forms), and the potential energy. All the energy are expressed in MeV. The experimental value of the energy for the external neutrons is  $-34.407 \text{ MeV}$ .

Force	$E$	$E_{\text{kin}}^{jf}$	$E_{\text{kin}}^{pb}$	$E_{\text{pot}}$
I	-29.9(1)	142.6(3)	142.4(2)	-172.2(2)
II	-60.5(1)	123.5(2)	123.6(2)	-184.1(3)

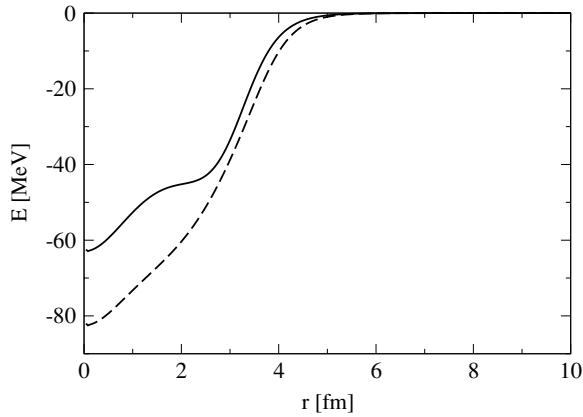


FIG. 1. Effective single-particle potential generated by the HF algorithm, with Skyrme's parameter of type Force I (full line) and Force II (dashed line).

because the two sets of Skyrme's parameters give quite different effective-HF potentials (as plotted in Fig. 1). As a criterion for determining which shell (and which set of orbitals) to use, we chose to minimize the difference between  $\langle H \rangle$  and the available experimental estimates of the binding energy of the nucleus.

#### D. Computational Details

To have an accurate estimate of the ground-state energies of the isotopes, we performed several sets of runs for different values of the time-step and walker populations. The reported values are all extrapolated to  $\Delta\tau \rightarrow 0$ . Also, the dependence of the result from the number of walkers used was investigated. Some calculations were repeated for 500 and 1000 walkers. For relatively long time steps, the energy has rather large fluctuations when a smaller number of walkers is employed. On the other hand, the average energy does not show a clear trend outside the statistical fluctuations. Therefore we present all results obtained with 1000 walkers.

## IV. RESULTS

### A. Ground states

In Table III we report the AFDMC energies obtained for the isotopes series  $^{18}\text{O}$ – $^{22}\text{O}$  compared with the available experimental values. As expected, the computed values are quite different from the experiment, although the relative

TABLE III. Ground-state energy calculated with AFDMC. All the energies are expressed in MeV.

Isotope	$E_{\text{AFDMC}}$	$E_{\text{exp}}$
$E_{^{18}\text{O}}$	−18.04(2)	−12.188
$E_{^{19}\text{O}}$	−22.4(1)	−16.145
$E_{^{20}\text{O}}$	−29.36(6)	−23.752
$E_{^{21}\text{O}}$	−33.6(2)	−27.558
$E_{^{22}\text{O}}$	−40.48(5)	−34.407

TABLE IV. Ground-state energy calculated with AFDMC. We report the differences between the isotopes we had studied. All the energies are expressed in MeV.

Isotope	$E_{\text{AFDMC}}$	$E_{\text{exp}}$
$E_{^{19}\text{O}} - E_{^{18}\text{O}}$	−4.4(1)	−3.957
$E_{^{20}\text{O}} - E_{^{18}\text{O}}$	−11.32(8)	−11.564
$E_{^{21}\text{O}} - E_{^{18}\text{O}}$	−15.5(2)	−15.370
$E_{^{22}\text{O}} - E_{^{18}\text{O}}$	−22.44(7)	−22.219

discrepancy never exceeds 30%. Of course this is a drawback of the use of an external potential for including the effects of the filled core of the nucleus. In particular the total binding energies are all overestimated. This reflects the absence of a correct description of the density of neutrons at the center of the drop, which is underestimated, giving rise to an effective potential that is too deep for small distances from the center. Moreover we completely neglect core-polarization effects. However, one can obtain most of the information needed to understand the effects of  $NN$  interaction in the external shell by looking at energy differences between the isotopes considered. In fact, if the intrashell interaction has a dominant effect, the gaps should not depend too much on the quality of the external well considered. In Table IV and in Fig. 2 we report the energy differences for the isotopes considered compared with the corresponding differences obtained from the experimental results. Our calculations have also been compared with the GFMC results reported in Chang *et al.* [7]. As can be seen, in this case the agreement between computed and experimental values is excellent. It has to be noted that for the  $^{19}\text{O}$  ground state we mixed two orbitals with the same angular momentum  $1D_{5/2}$  and the  $1D_{3/2}$ ; this is the only way to obtain the correct energy. In fact, the same calculation with a wave function restricted to only one orbital, as for all other isotopes, gives an energy of  $-19.64(5)$  MeV, instead of the deeper value of  $-22.4(1)$  MeV. This indicates that, for this state, which is an odd nucleus, components of higher single-particle states are very important.

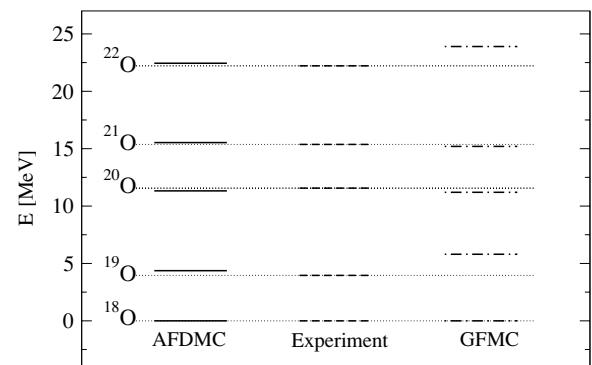


FIG. 2. Outline of differences between energies of the isotope series studied. All the energies are expressed in mega-electron-volts, and all values are referred to that of  $^{18}\text{O}$ . Results are compared with experimental results and with GFMC calculations [7].

It is also possible to note how the binding energy of  $^{22}\text{O}$  relative to  $^{18}\text{O}$  is almost coincident with the experimental finding in the AFDMC, while one has again a strong overestimation in the GFMC calculation. This is quite surprising, as  $^{22}\text{O}$  is a closed-shell nucleus. However, it is possible that in this case the choice of the self-consistent HF potential gives a better description of the outer shell than the all-neutron picture used in the GFMC calculations.

The isotope  $^{17}\text{O}$  is a particular case. In fact this nucleus has only one valence neutron, and no calculation is needed to determine the energy, which is given by the eigenvalue of the single particle problem solved in the external well. The energy of the  $^{17}\text{O}$  is  $-3.89(1)$  MeV. This value reasonably compares with the experimental binding energy of  $-4.144$  MeV. The difference between the two values partly accounts for the total absence of a realistic interaction between the external neutron and the core. The missing correlations may describe very important effects like core polarization, spin-orbit interaction, and pairing between internal neutrons and an external one; instead these effects are partially included with the HF well and by AFDMC calculations with more external neutrons.

In Fig. 3 we report the AFDMC densities normalized to unity of the external neutrons for the isotopes considered in this work. As can be seen, the neutron's densities are all quite similar, and very small deviations are present. In fact, the density profile seems to be larger when there are more neutrons; this can be expected because of the repulsive nature of the  $n$ - $n$  interaction. In the figure we also display the density of  $^{16}\text{O}$  calculated with Skyrme's interaction to make evident the "halo" effect of the external neutrons.

### B. Excited states

By construction of the appropriate wave functions it is possible to study the low-lying excited states of a given isotope. Excited states were computed for the isotopes  $^{18}\text{O}$  and  $^{21}\text{O}$ . We limited ourselves to states that can be built while still remaining within the  $1D_{5/2}$  shell. No modification of the algorithm is

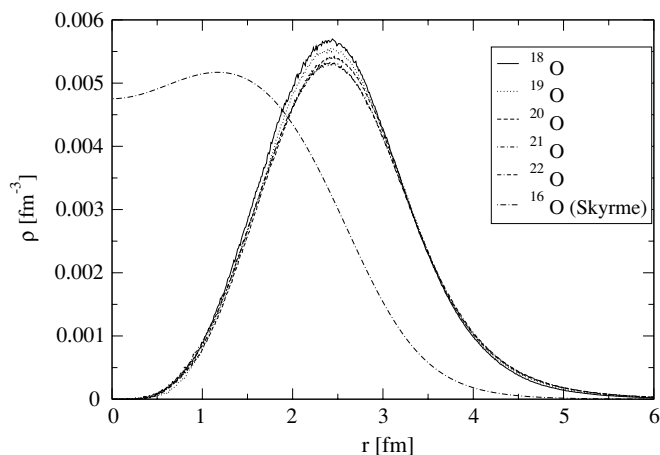


FIG. 3. Radial densities of external neutrons for all isotopes in the ground state calculated with AFDMC and the Skyrme's density of  $^{16}\text{O}$ .

TABLE V. Excitation energy calculated with AFDMC of the isotopes  $^{18}\text{O}$  and  $^{21}\text{O}$  compared with experimental results (see text). All energies are in MeV.

Isotope	State	$\Delta E_{\text{AFDMC}}$	$\Delta E_{\text{exp}}$
$^{18}\text{O}$	$2^+$	1.99(9)	2.0(2)
	$4^+$	5.08(2)	3.6(2)
$^{21}\text{O}$	$1/2^+$	1.24(9)	1.218(4)
	$3/2^+$	2.11(9)	2.133(5)

required. If the states considered are orthogonal to the ground state, the projected wave function will be constrained within the same subspace. We report in Table V the AFDMC results compared with experimental results of Norum *et al.* [26] for  $^{18}\text{O}$  and of Stanoiu *et al.* [1] for  $^{21}\text{O}$ .

In Fig. 4 we show the results for the  $^{18}\text{O}$  isotope compared with experiment and with multideterminant projection Hartree-Fock (MDHF) results by Morrison *et al.* [27].

The excitation energy of the  $2^+$  state turns out to be in excellent agreement with the experimental findings. The situation for the  $4^+$  state is much less satisfactory. There are essentially two possible sources for this discrepancy. In the case of the  $J = 4$  state, the large angular momentum might give the spin-orbit component of the potential a relevant role. The presence of spin-orbit terms tends to heavily modify the nodal structure of the wave function. In particular, it was recently shown by Brualla *et al.* [28] that the nodal structure of the homogeneous neutron liquid is much improved when explicit backflow effects are introduced into the determinantal part of the wave function. It is possible that a similar effect might be observed here.

The excitation energies for the  $^{21}\text{O}$  isotope are shown in Fig. 5. We compare our AFDMC results with experiments and with shell-model calculations by Brown [29]. In this case the agreement between AFDMC results and experiments is very good for all the states considered.

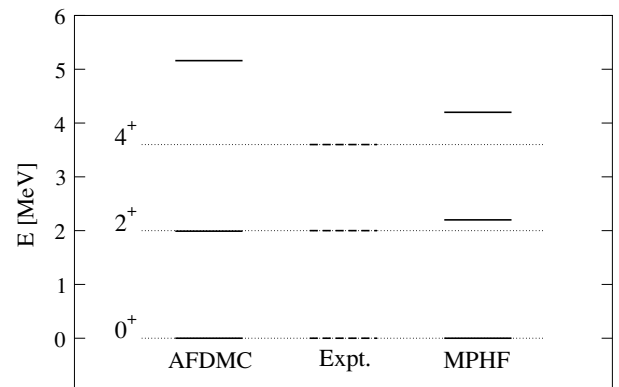


FIG. 4. Low-lying excitation energies of the  $^{18}\text{O}$  isotope compared with experimental values from Ref. [26]. All energies are in mega-electron-volts. Results are compared with MDHF results of Ref. [27].

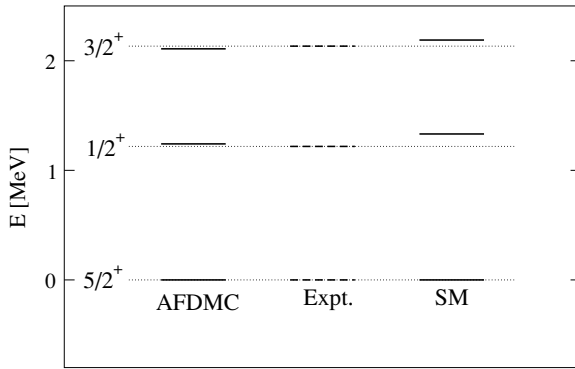


FIG. 5. Low-lying excitation energies of the  $^{21}\text{O}$  isotope compared with experimental values from Ref. [1]. All energies are in mega-electron-volts. Results are compared with the shell-model results of Ref. [29].

## V. CONCLUSIONS

We used the AFDMC method to study properties of off-shell neutrons in oxygen isotopes, including a realistic  $NN$  potential. The approximate treatment of the  $^{16}\text{O}$  core as an external potential well computed by the HF method does not compromise at all the quality of the result for the energy differences between isotopes in the  $1D_{5/2}$  (and in the  $1D_{3/2}$  in the case of  $^{19}\text{O}$ ) shell. The same procedure was applied to the computation of low-lying excited states in  $^{18}\text{O}$ . When a more significant deviation with respect to the experimental results

is present, it can be attributed to the low-quality description of the nodal structure of the nucleus, which enters the calculation through the constrained path approximation. Results confirm that the  $NN$  interaction is dominant with respect to mean-field effects in determining the structure of the energy levels of the external neutrons. Calculations within the same scheme could be extended to the case of F and Ne isotopes for which experimental results are available. It is also possible, by the addition of the contribution from the  $2S_{1/2}$  shell, to move up to the drip line. This, however, implies a better treatment of the effective potential well near the center of the nucleus. In fact, a plain inclusion of  $S$  neutrons in the present calculation would lead to a jump in the binding energy because the neutron density in the center of the nucleus is not well treated. Work in this direction is in progress.

## ACKNOWLEDGMENTS

We thank S. a Beccara for providing us the Clebsch-Gordon (CG) coefficients for the  $^{19}\text{O}$  states. We also thank G. Orlandini and W. Leidemann for useful discussions about the problem. Calculations were partly performed on the Advanced Linux Parallel System (ALPS) cluster at European Center for Theoretical Studies in Nuclear Physics and related Areas (ECT\*) in Trento, and partly at CINECA through an INFN/DEMOCRITOS grant. Partial funding by INFN is acknowledged. K. E. Schmidt is partially supported by the U.S. National Science Foundation through grant PHY-0456609.

- [1] M. Stanoiu, F. Azaiez, Z. Dombrádi, O. Sorlin, B. A. Brown, M. Bellegruic, D. Sohler, M. G. S. Laurent, M. J. L. Jimenez, Y. E. Penionzhkevich *et al.*, Phys. Rev. C **69**, 034312 (2004).
- [2] M. Thoennessen, T. Baumann, J. Enders, N. H. Frank, P. Heckmann, J. P. Seitz, A. Stolz, and E. Tryggestad, Nucl. Phys. **A722**, 61c (2003).
- [3] A. Leistenschneider, T. Aumann, K. Boretzky, L. F. Canto, B. V. Carlson, D. Cortina, U. D. Pramanik, T. W. Elze, H. Emling, H. Geissel *et al.*, Phys. Rev. C **65**, 064607 (2002).
- [4] A. T. Reed, O. Tarasov, R. D. Page, D. Guillemaud-Mueller, Y. E. Penionzhkevich, R. G. Allatt, J. C. Angélique, R. Anne, C. Borcea, V. Burjan *et al.*, Phys. Rev. C **60**, 024311 (1999).
- [5] H. Nakada, Nucl. Phys. **A722**, 117c (2003).
- [6] M. Kimura and H. Horiuchi, Nucl. Phys. **A722**, 507c (2003).
- [7] S. Y. Chang, J. Morales, Jr., V. R. Pandharipande, D. G. Ravenhall, J. Carlson, S. C. Pieper, R. B. Wiringa, and K. E. Schmidt, Nucl. Phys. **A746**, 215 (2004).
- [8] K. E. Schmidt and S. Fantoni, Phys. Lett. **B446**, 93 (1999).
- [9] H. Masui, T. Myo, K. Kato, and K. Ikeda, Nucl. Phys. **A722**, 469c (2003).
- [10] A. Hasegawa and S. Nagata, Prog. Theor. Phys. **45**, 1786 (1971).
- [11] A. B. Volkov, Nucl. Phys. **74**, 33 (1965).
- [12] W. M. C. Foulkes, L. Mitas, R. J. Needs, and G. Rajagopal, Rev. Mod. Phys. **73**, 33 (2001).
- [13] R. B. Wiringa, V. G. J. Stoks, and R. Schiavilla, Phys. Rev. C **51**, 38 (1995).
- [14] R. B. Wiringa, Argonne  $v_{18}$  and  $v_8^{\prime}$  Potential Package (1994): <http://www.phy.anl.gov/theory/research/av18/av18pot.f>
- [15] S. C. Pieper, V. R. Pandharipande, R. B. Wiringa, and J. Carlson, Phys. Rev. C **64**, 14001 (2001).
- [16] B. S. Pudliner, V. R. Pandharipande, J. Carlson, S. C. Pieper, and R. B. Wiringa, Phys. Rev. C **56**, 1720 (1997).
- [17] A. Akmal and V. R. Pandharipande, Phys. Rev. C **56**, 2261 (1997).
- [18] A. Sarsa, S. Fantoni, K. E. Schmidt, and F. Pederiva, Phys. Rev. C **68**, 024308 (2003).
- [19] S. Fantoni, A. Sarsa, and K. E. Schmidt, Phys. Rev. Lett. **87**, 181101 (2001).
- [20] F. Pederiva, A. Sarsa, K. E. Schmidt, and S. Fantoni, Nucl. Phys. **A742**, 255 (2004).
- [21] S. Fantoni, A. Sarsa, and K. E. Schmidt, Prog. Part. Nucl. Phys. **44**, 63 (2000).
- [22] R. B. Wiringa, V. Fiks, and A. Fabrocini, Phys. Rev. C **38**, 1010 (1988).
- [23] D. Vautherin and D. M. Brink, Phys. Rev. C **5**, 626 (1972).
- [24] H. J. Jackson and E. Feenberg, Ann. Phys. (NY) **15**, 266 (1961).
- [25] V. R. Pandharipande and H. A. Bethe, Phys. Rev. C **7**, 1312 (1973).
- [26] B. E. Norum, M. V. Hynes, H. Miska, W. Bertozzi, J. Kelly, S. Kowalsky, F. Rad, C. P. Sargent, T. Sasanuma, W. Turchinetz *et al.*, Phys. Rev. C **25**, 1778 (1982).
- [27] I. Morrison, R. Smith, P. Nesci, and K. Amos, Phys. Rev. C **17**, 1485 (1978).
- [28] L. Brualla, S. Fantoni, A. Sarsa, K. E. Schmidt, and S. A. Vitiello, Phys. Rev. C **67**, 065806 (2003).
- [29] B. A. Brown, Prog. Part. Nucl. Phys. **47**, 517 (2001).